REVIEW ARTICLE
PUBLISHED ONLINE: 29 JULY 2012 | DOI: 10.1038/NGEO1521
nature geoscience

Possible links between long-term geomagnetic variations and whole-mantle convection processes

A. J. Biggin[1]*, B. Steinberger[2,3], J. Aubert[4], N. Suttie[1], R. Holme[1], T. H. Torsvik[3,5,6], D. G. van der Meer[7,8] and D. J. J. van Hinsbergen[3]

The Earth's internal magnetic field varies on timescales of months to billions of years. The field is generated by convection in the liquid outer core, which in turn is influenced by the heat flowing from the core into the base of the overlying mantle. Much of the magnetic field's variation is thought to be stochastic, but over very long timescales, this variability may be related to changes in heat flow associated with mantle convection processes. Over the past 500 Myr, correlations between palaeomagnetic behaviour and surface processes were particularly striking during the middle to late Mesozoic era, beginning about 180 Myr ago. Simulations of the geodynamo suggest that transitions from periods of rapid polarity reversals to periods of prolonged stability — such as occurred between the Middle Jurassic and Middle Cretaceous periods — may have been triggered by a decrease in core–mantle boundary heat flow either globally or in equatorial regions. This decrease in heat flow could have been linked to reduced mantle-plume-head production at the core–mantle boundary, an episode of true polar wander, or a combination of the two.

The Earth's magnetic field exhibits internally driven variations on an extremely wide range of timescales[1]. As a highly nonlinear system, the geodynamo could produce all of these through a stochastic process without the need to invoke any external forcing mechanism[1–3]. For variations observed on the timescale of tens to hundreds of millions of years (Myr)[4,5], however, the similarity to mantle convection timescales suggests an alternative hypothesis, whereby changes in core–mantle boundary (CMB) heat flow play an important role in determining average geomagnetic behaviour. This forcing could combine with a further stochastic component of geodynamo behaviour, and is worthy of intense investigation because it could potentially allow geomagnetic behaviour to be used to constrain lowermost mantle processes occurring over Earth's history. An overarching theory of interaction could then be developed between the two great engines of the Earth's interior: the geodynamo and mantle convection incorporating plate tectonics.

Based on the a priori acceptance of the mantle forcing hypothesis, numerous researchers have causally related events in the palaeomagnetic and geological records[6–19], linking, for example, changes in magnetic polarity reversal frequency, through mantle plumes, to the emplacement of large igneous provinces. Such claims are somewhat speculative, but their general concept is plausible. Interpretations of seismic wave tomography using global plate reconstructions suggest that sinking lithospheric slabs and rising mantle plumes are indeed whole-mantle processes[20,21] conceivably influencing both the geodynamo and the surface. Furthermore, numerical geodynamo models strongly support claims made by palaeomagnetists[22–24], that persistent non-axial dipole features of the geomagnetic field observed over the last 10 kyr, and during individual excursions and reversals, reflect the influence of the present-day pattern of core–mantle heat flow[25,26]. Mechanisms other than thermal interactions across the CMB could also force the geodynamo on these and other timescales[27], but we shall not focus on these for the purpose of this review.

Here we present a synthesis of the latest results from a variety of disciplines, to examine possible causal relationships between geomagnetic behaviour and mantle processes on the 10–100 Myr timescale. We also highlight the future research required to test and develop these links.

Geomagnetic variations on the 10–100 Myr timescale

Two measures of geomagnetic behaviour are considered here: reversal frequency refers to the average rate with which geomagnetic field flips from apparently stable normal to reverse polarity and vice versa; dipole moment is the inferred strength of the dominant dipole component of the geomagnetic field.

The geomagnetic polarity timescale[28–32] (Fig. 1) indicates that reversal occurrence is a stochastic process, but also provides unequivocal evidence that the average reversal frequency has varied considerably over the last few hundreds of Myr[5]. Numerous statistical analyses of this record have failed to produce a consensus on the underlying statistical distribution or resolve whether a stationary dynamo process could produce such a time-dependent pattern of reversal occurrence. We restrict ourselves to investigating the coarsest (>30 Myr) timescale variations, as these are most readily explained in terms of mantle convection processes.

The earliest parts of the marine magnetic anomaly record (Fig. 1a) cannot be straightforwardly interpreted in terms of a reversal sequence, but continental magnetostratigraphic studies suggest that anomalies back to at least 160 Myr ago are indeed

[1]Geomagnetism Lab, Geology and Geophysics, School of Environmental Sciences, University of Liverpool, L69 7ZE, UK, [2]Helmholtz Centre Potsdam, GFZ German Research Centre for Geosciences, 14473 Potsdam, Germany, [3]Physics of Geological Processes, University of Oslo, Sem Saelands vei 24, 0316 Oslo, Norway, [4]Institut de Physique du Globe de Paris, UMR7154, INSU, CNRS – Université Paris-Diderot, PRES Sorbonne Paris Cité, 1 rue Jussieu, 75238 Paris cedex 5, France, [5]Center for Geodynamics, Geological Survey of Norway (NGU), Leiv Eirikssons vei 39, 7491 Trondheim, Norway, [6]School of Geosciences, University of the Witwatersrand, WITS 2050 Johannesburg, South Africa, [7]Institute of Earth Sciences, Utrecht University, Budapestlaan 4, 3584 CD Utrecht, The Netherlands, [8]Nexen Petroleum UK Ltd., Charter Place, UB8 1JG, Uxbridge, UK.
*e-mail: biggin@liv.ac.uk

associated with reversals[33,34]. Two periods in the last 200 Myr seem to represent examples of the most extreme geomagnetic behaviour observed so far (Fig. 1): the Middle–Late Jurassic (around 150–170 Myr ago) when reversal frequency peaked[29,33], possibly in excess of 12 Myr^{-1}; and the Cretaceous Normal Superchron (CNS; 84–121 Myr ago) when the field was almost exclusively of single polarity for a period spanning nearly 40 Myr[35,36]. In the late Cainozoic, some of the polarity chrons are of shorter duration than have been documented at any earlier time. The density of short (<0.2 Myr) chrons was clearly higher in the Middle Jurassic, however, leading to higher average reversal frequency, even before considering that short duration chrons are more likely to have been overlooked in earlier time periods.

Variations in the mean dipole moment through the Cretaceous and Cainozoic are still the subject of vigorous debate[37–41] and good quality data from earlier times are sparse. Nonetheless, measurements of dipole moment made from both whole-rock and single silicate crystals, together with interpretations of the marine magnetic anomaly record, all suggest that the average dipole moment was lower than average for at least part of the Jurassic period (140–200 Myr ago; Fig. 1b)[6,29,38,42–46].

Reversal frequency and dipole moment records suggest that there was a major transition in geomagnetic behaviour between the Middle Jurassic (~170 Myr ago) and the Middle Cretaceous (~120 Myr ago; Fig. 1). Records of palaeosecular variation analysis, although based on limited data in the case of the earlier time period, also support significantly different geomagnetic behaviour during the Jurassic and Middle Cretaceous[47]. It is still debated whether this transition from hyper-reversal activity to superchron occurred over a short (~3 Myr) or much longer (~40 Myr) time period[2,48].

Two earlier Phanerozoic superchrons have been claimed from continental magnetostratigraphic records (see Fig. 1b): the Permo-Carboniferous Reversed Superchron (PCRS; ~265–310 Myr ago[49]) and the Ordovician Reversed Superchron (ORS; ~460–490 Myr ago[50]). There is direct magnetostratigraphic evidence that reversal frequency was very high (>7–10 Myr^{-1}) just 10–20 Myr before the ORS in the Middle Cambrian[51,52]. Magnetostratigraphic data are lacking before the PCRS but preliminary measurements of the virtual dipole moment in the Devonian and Silurian periods are lower than average[6], similarly to those in the Jurassic when reversal frequency was high. Therefore, the CNS, PCRS and ORS may all have been preceded by a period of reversal hyperactivity. Interestingly, a further sharp transition from high reversal frequency to superchron behaviour has also been reported from before the Phanerozoic in late Mesoproterozoic (~1000–1060 Myr ago) rocks from southeastern Siberia[53].

In summary, palaeomagnetism supports geomagnetic variations occurring on the 10–100 Myr timescale throughout the Phanerozoic and possibly also in the Precambrian. Furthermore, Fig. 1b suggests some periodicity in the reversal record, each superchron separated by a period of 180–190 Myr.

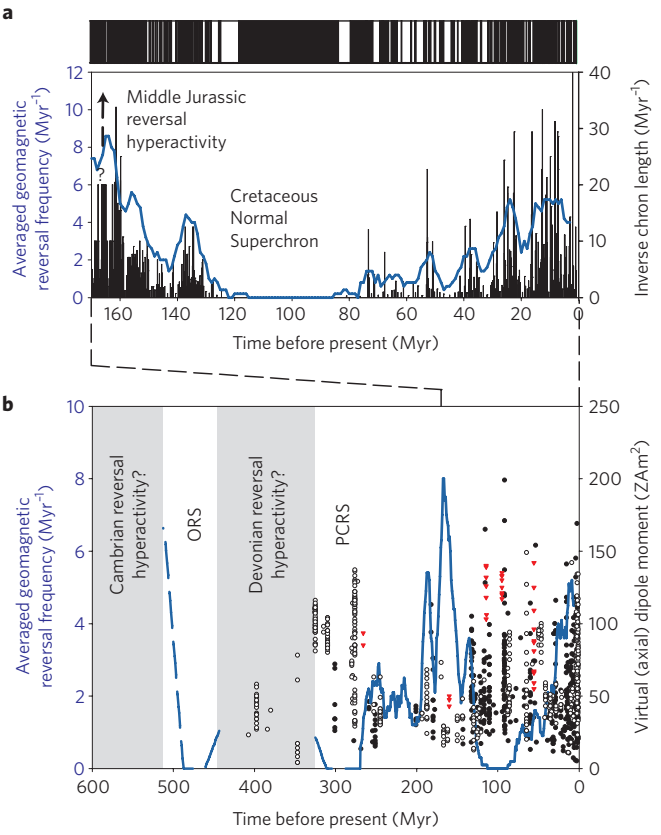

Figure 1 | Records of geomagnetic polarity reversal frequency and dipole moment since the Cambrian period. a, The marine magnetic anomaly record (MMA)[28–31] and plots of inverse chron length (black bars) and reversal frequency (10 Myr running mean; blue line). **b**, Reversal frequency from the MMA and magnetostratigraphic studies[33] (shaded area indicates insufficient data) alongside virtual (axial) dipole moment (spatially normalized field intensity) measurements[97] from single silicate crystals (red triangles) and whole rocks (filled circles for Thellier[98] or microwave methods[99] with pTRM checks and the LTD-DHT Shaw[100] method; open circles for other methods; $N \geq 3$; $\sigma/\mu \leq 0.25$ in all cases). ORS, Ordovician Reversed Superchron; PCRS, Permo-Carboniferous Reversed Superchron.

Sensitivity of the geodynamo to changes in CMB heat flow

To understand how geomagnetic variations could be related to changes in CMB heat flow, we turn to insights provided by dynamo theory. Numerical geodynamo models provide powerful tools with which to study geomagnetic variations on all timescales, but, because the parameters at which numerical dynamos can be operated differ enormously from those of the Earth's core, systematic exploration of parameter space is necessary. In particular, the very large disparity between the typical diffusion times of the core momentum, magnetic field and buoyancy anomaly, and the ratios of all these times with respect to an Earth day, must be greatly reduced in the models to maintain a tractable problem size[25].

As fluid flow in the outer core (measured in mm s^{-1}) is so much faster than mantle flow (measured in mm yr^{-1}), the geodynamo is sensitive to the 'instantaneous' heat flow conditions imposed by the mantle rather than its rate of change on mantle timescales. The geodynamo is largely driven by compositional convection produced by the release of light elements at its base rather than thermal convection caused by cooling from the top. Nonetheless, this process is still dependent on, and modulated by, the heat flowing out of the core at a rate dictated by conditions in the lowermost mantle.

To first order, reversal frequency seems to be positively correlated to CMB heat flow: enhancing convection in dynamo simulations by increasing this flow tends to destabilize the dipole generation process, making reversals more likely[54–57], although maintaining a stochastic pattern[56]. Reversing dynamos require high forcing and long simulation times for a significant statistical assessment, however, making extensive parametric studies difficult[58].

The evolution of reversal frequency has been linked to a local version of the Rossby (Ro) number (the ratio of inertial to rotational forces), which is specific to a typical length scale of the fluid flow[54,55,59,60]. An empirically derived relationship[54,59] suggests that the local Ro scales as the square root of the power available to drive the dynamo (which increases with CMB heat flow). Results from a simple numerical dynamo model[55] suggests that a twofold increase

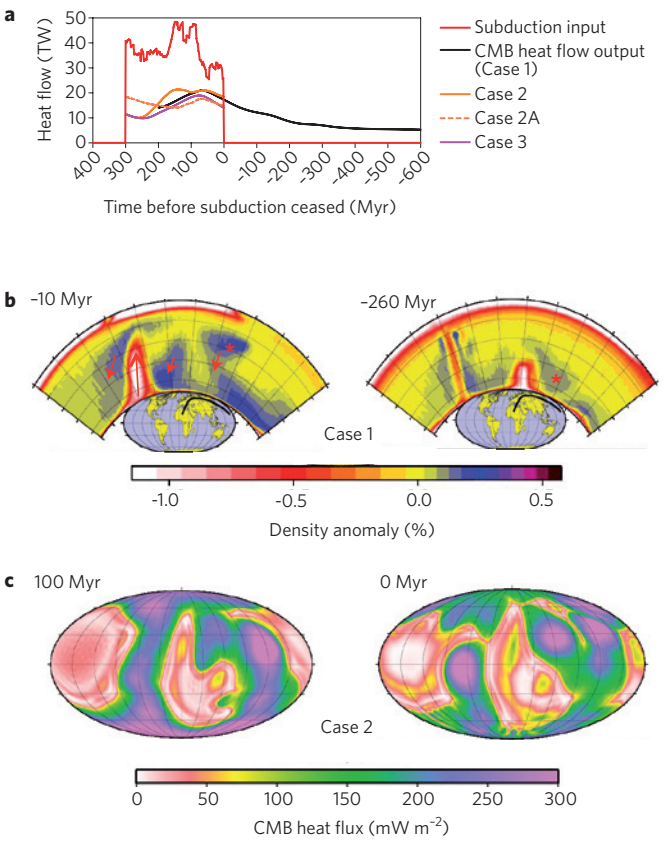

Figure 2 | Representative cases of a mantle flow model showing the effects of subducted slabs on core–mantle boundary (CMB) heat flow. a, CMB heat flow increases ~50 Myr after subduction begins (cases 2 and 3) but is still decreasing ~300 Myr after subduction ends (case 1). **b**, The slab (blue) marked with the asterisk interacts with a plume (red and white) and remains as a positive density anomaly after 250 Myr. **c**, Present-day CMB heat flow (reversal frequency ~4 Myr^{-1}) is greater at equatorial latitudes and more asymmetric about the equator than during the superchron 100 Myr ago.

of the local Ro number (associated with a fourfold increase in dynamo power according to the scaling relationship) is sufficient to drive the dynamo from a state in which reversals first occur to a state in which they occur frequently at an average rate of about 10 every million years. Accounting for the affine relationship between dynamo power and CMB heat flow[54], this increase in the reversal frequency can, for example, be achieved if the CMB heat flow varies from 4 TW to 12 TW in a system where the core adiabatic heat flow is 6 TW, or from 9 to 20 TW in a system where the adiabatic heat flow is 15 TW (ref. 60).

When increasing the CMB heat flow beyond the point at which reversals start, the magnetic field strength may decrease. Results from a simple numerical dynamo model[55] suggest that a twofold increase in the CMB heat flow could reduce the dipole moment by half. Assuming that the geodynamo lies close to such a transition[55,61], a period of dynamo hyperactivity (high reversal frequency) — caused by high CMB heat flow — may be associated with a low dipole moment, and a period of low dynamo activity (superchron) — caused by low CMB heat flow — may be characterized by a high dipole moment[56]. This is consistent with the combination of low dipole moment and high reversal frequency measured in the Jurassic. The opposite combination (high dipole moment, no reversals) is suggested by some data[45] during the Cretaceous Superchron (Fig. 1b) and would also fit this prediction.

Changes in the spatial pattern of CMB heat flow alone may also exert a strong effect on reversal frequency[26,62]. It has been argued[63] that increasing the heterogeneity of the CMB heat flow, while holding the net heat flow at a constant value, also tends to decrease the stability of the dynamo, thereby producing more reversals. Due to the nature of its columnar convection, the geodynamo is expected to be mostly influenced by low-latitude heat-flow variations[25], and this sensitivity has been highlighted in a numerical model study[63] in which many more reversals occurred when the low-latitude heat flow was increased. Using a mechanism developed from a low-order dynamo model[64], it has also been argued that the equatorial asymmetry in CMB heat flow has strongly influenced reversal frequency: reversals become more common when the north–south symmetry is broken[14].

Intriguingly, the outputs of some heterogeneously forced models[63] do not seem to produce a simple inverse relationship between measured average reversal frequency and mean axial dipole moment. If confirmed as a robust prediction of geodynamo theory, a decoupling of these parameters under certain heterogeneous boundary conditions could provide an explanation, alternative to low measurement fidelity[40], for the apparent small change in mean dipole moment since the Middle Cretaceous (Fig. 1b).

Overall, dynamo theory supports the hypothesis that the geomagnetic variability outlined in the previous section could be caused by changes in the magnitude and/or spatial pattern of heat flow across the CMB, with higher heat flow (particularly in equatorial zones) and greater pattern heterogeneity both producing more reversals. Although significant variations in chron length have been observed to occur spontaneously in a long-running dynamo simulation[65], those of the magnitude observed in the palaeomagnetic record have not been reproduced without forcing[56]. To our knowledge, no geodynamo modelling studies have yet explicitly tested how the effects of changing the global net heat flow differ in the cases of homogeneous versus heterogeneous boundary conditions. As the following section makes clear, this is urgently required to understand how long-timescale geomagnetic variations might arise.

CMB heat flow and its temporal variability

Heat flow from the core into the mantle is proportional to the temperature contrast across the thermal boundary layer (TBL) at the base of the mantle and the thermal conductivity of the lowermost mantle, and inversely proportional to the TBL's thickness. All of these quantities, however, are rather uncertain, and therefore estimates of present-day heat flow are widely discrepant (although mostly in the range 5–15 TW (ref. 66); 33–100 m Wm^{-2}). Seismological studies suggest a high degree of heterogeneity in the lowermost mantle[67], which probably corresponds to large variations in local heat flow. In particular, two approximately antipodal large low shear-wave velocity provinces span thousands of kilometres under Africa and the central Pacific, and are thought to represent intrinsically dense thermochemical piles that may be associated with very low CMB heat flow[68].

CMB heat flow is likely to be variable on mantle convection timescales[15]. The TBL may be influenced by subducted slabs in the lower mantle, by mantle plumes departing from the CMB, and by the distribution of the thermochemical piles in the lowermost mantle. Furthermore, episodes of true polar wander (TPW) effectively rotate the entire pattern of CMB heat flow with respect to the dominant time-averaged flow structures in the outer core.

Mantle flow models constrained by plate reconstructions at their upper boundary can be used to infer the history of CMB heat flow and its relationship with subduction history[15]. This approach is applied here using an independent set of mantle flow models with a somewhat different radial viscosity profile, subduction history and model parameters than previous efforts (see supplementary information for details). These models mostly support a large spatial variation in the amplitude of CMB heat flux. Beneath

thermochemical piles (mostly red-white colours in Fig. 2c), it is much lower (<40 m Wm^{-2}) than where subducted slab remnants overlie the CMB (150–250 mWm^{-2})[15]. Reconstructed positions of large igneous provinces and kimberlites suggest that the thermochemical piles have covered similar areas of the CMB for over 500 Myr[20]. Large variations in CMB heat flow must therefore have occurred elsewhere.

Our mantle flow models mostly produce high total CMB heat flow (>10 TW) as may be required to maintain the geodynamo[60]. Case 2A (using the output of case 2 at 0 Myr as the initial condition) in Fig. 2 is the closest to equilibrium and produces temporal variations in total CMB heat flow on the order of a few tens of percent over the last few hundreds of Myr (see Supplementary Movie S1). According to the empirical scaling relationship[54,59] mentioned earlier, relative changes of this magnitude would probably be insufficient to drive significant changes in the reversal behaviour of a homogeneously forced dynamo[54]. The boundary conditions for the geodynamo are probably far from the homogeneous state used to construct this relationship, however, and dynamo models also supports changes in magnetic behaviour forced purely by changes in the pattern of heat flow, even when no net variation occurs[26,62,63]. Therefore, we conclude that, although the concepts under review here presently lack quantitative support, the possibility that changes in CMB heat flow do affect the geodynamo cannot yet be rejected. The highly nonlinear nature of the geodynamo could plausibly amplify even relatively minor shifts in forcing to produce major transitions in geomagnetic behaviour.

Potential links with subduction activity

Numerous studies have attempted to relate the distribution of subduction zones and inferred subduction rates to variations in geomagnetic behaviour. Some of their hypotheses[6,9,69] now seem unlikely because they assume that increasing net CMB heat flow decreases reversal frequency (and increases mean dipole moment), the opposite relationship to that implied by the dynamo models. Others do invoke more plausible relationships between CMB heat flow and dynamo behaviour but allow no time lag in transferring information between the crust and core[10,14].

Sinking lithospheric slabs can stagnate temporarily on top of the 660 km discontinuity[70], but they eventually sink into the lower mantle[71–74]. Sinking slabs displace material ahead of them, thinning the TBL and increasing CMB heat flow long before they actually reach the lowermost mantle[75]. By running some of our models with zero subduction flow before and after the 0–300 Myr period for which the plate history is constrained, the time delay associated with the response of CMB heat flow to slab input was explored. The models showed an initial response to subduction initiation after a delay of approximately 50 Myr (Fig. 2a). By contrast, the time between subduction cessation and heat flow decrease at the location where the slab perturbed CMB heat flow can be 250 Myr or longer, as the slab sinks and is subsequently warmed (Fig. 2). Similarly, a study that coupled tomography to plate reconstructions found a survival time for slabs of ~250–300 Myr[21].

Some mantle models[15] have produced weak minima in the equatorial heat flow at times (around 100 Myr and 270 Myr ago) that fall within the CNS and PCRS. This, combined with an apparent sensitivity of dynamo models[63] to variations in this parameter, has been offered as a potential explanation for the occurrence of these superchrons[15]. However, our models do not all support a minimum in equatorial CMB heat flow at the time of the last superchron (see Supplementary Information).

A more robust observation based on our analysis is that equatorial asymmetry increased from a minimum in the Cretaceous as subduction flux in the northern hemisphere increased relative to that in the south (Fig. 2c and Supplementary Fig. S1). This suggests that increasing north–south asymmetry in heat flow might

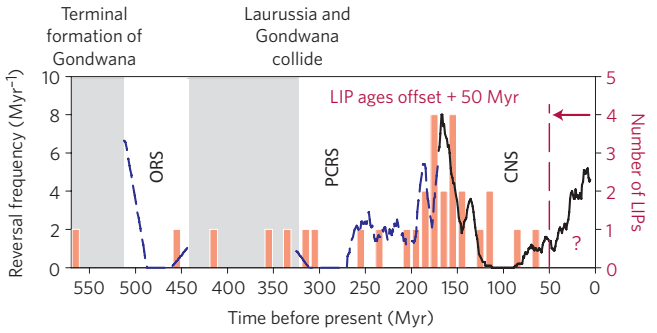

Figure 3 | Average reversal frequency and eruption ages[20] of large igneous provinces (LIPs; offset by +50 Myr) that have not yet been subducted. Mantle plume heads leaving the CMB may reflect enhanced heat flow out of the core, potentially increasing reversal frequency tens of Myr before the resulting eruption of the LIPs. Allowing for an average rise-time of 50 Myr results in a broad correlation that would associate geomagnetic reversal hyperactivity in the Middle Jurassic with widespread LIP emplacement in the Middle Cretaceous. In the period 0–50 Myr, mantle plume heads that had left the CMB would not yet have reached the surface. ORS, Ordovician Reversed Superchron; PCRS, Permo-Carboniferous Reversed Superchron; CNS, Cretaceous Normal Superchron.

have played a role in increasing reversal frequency through the late Cretaceous and Cainozoic[14], although the required sensitivity of the dynamo remains to be established.

It has been argued[15] that the onset of the PCRS was essentially caused by the cessation of subduction associated with the collision of Laurussia and Gondwana approximately 20 Myr earlier, at 330 Myr ago. It is, however, not clear how this could fit with our findings of a long drawn-out response of CMB heat flow to subduction cessation (Fig. 2). Variability in slab sinking speeds[76] and CMB heat flow response time (Fig. 2) imply that establishing robust correlations between geomagnetic behaviour and subduction events may prove difficult.

Potential links mantle plume activity

Deep mantle plumes, rising from the lowermost mantle, remove hot material from the TBL, increasing the local CMB heat flow. This increase may be only a minor effect relative to the heat flow variations caused by the arrival of cold slabs above the CMB, however[77–79]. Our numerical model contains both slabs and plumes and supports that the departure of plume heads from the TBL is itself modulated to some degree by slab arrival. The margins of the thermochemical piles have been referred to as 'plume-generation zones' where plumes seem to form preferentially[20,80,81]. Here, slabs can act as a 'push broom', sweeping up material into upwellings over the margins of the piles[75,79,82,83] (Supplementary Fig. S3). Therefore, plume head departure from the CMB may be associated with an increase in heat flow there even if it does not directly cause it; the effects of slabs and plumes on CMB heat flow cannot easily be separated.

Early attempts to link mantle plume activity (expressed in the geological record as large igneous province and kimberlite formation) to magnetic reversal frequency claimed that plumes caused superchrons[11–13]. The Middle–Late Cretaceous was indeed a time of both major intra-plate volcanism (probably sourced by mantle plumes)[20,84] and unusually low geomagnetic reversal frequency, but it now seems unlikely that these two specific phenomena are directly related in the manner claimed. Dynamo models imply that plumes, and the increase in CMB heat flow they represent, are more likely to be associated with periods of elevated (rather than suppressed) reversal frequency[54,56,63]. Also, enhanced Cretaceous large igneous province (LIP) activity in both the African and

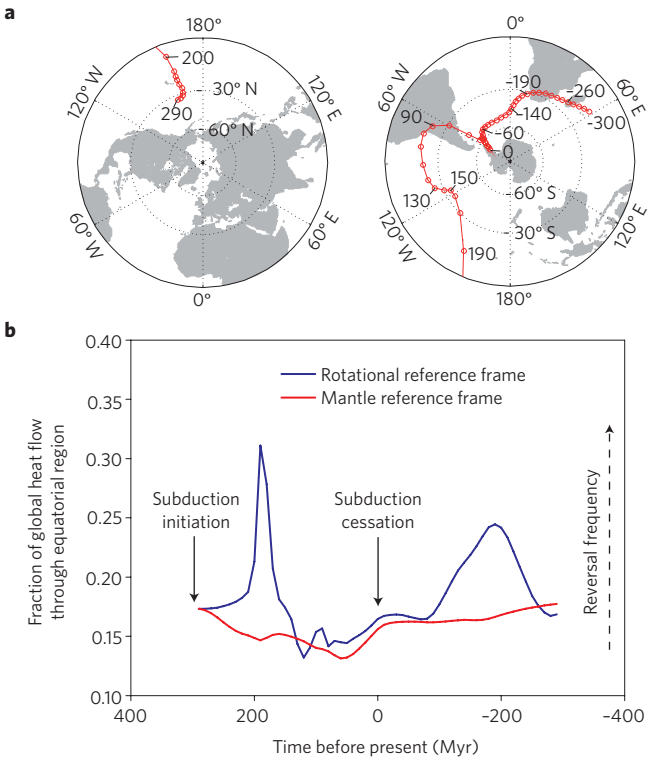

Figure 4 | True polar wander (TPW) as produced by a mantle flow model (case 2) subject to two major perturbations in subduction flux which affected the fractional CMB heat flow in the equatorial region. **a**, The geographic pole through time (Myr before present) shown on stereographic projections featuring present-day landmasses for reference. **b**, Time series of the fraction of global CMB heat flow between 10° N and 10° S. Differences between the heat flow in the two reference frames is due to TPW, which first maximizes and then minimizes its equatorial fraction, and could similarly affect reversal frequency.

Pacific hemispheres was apparently underway before the superchron even began[85], which would not allow time for the plumes to rise through the mantle.

It has also been claimed that the three Phanerozoic superchrons were each terminated by the departure of a plume head from the CMB, which then manifested itself in an LIP at the Earth's surface some 10–20 Myr later[8]. Such a short time lag works well for explaining superchron termination but leaves superchron onset unexplained and, assuming the same rise time, the Middle Cretaceous pulse of LIP activity uncorrelated with reversal frequency. Estimates for plume rise-time from the CMB to the surface vary between 5 and 100 Myr[86,87], with recent modelling[88] favouring 20–50 Myr. Taking the upper limit of 50 Myr suggests a broadly positive correlation between LIP activity and reversal frequency on the time range 50–200 Myr (Fig. 3), and one that is also consistent with our first-order understanding of how the geodynamo is likely to respond to changes in CMB heat flow.

The correlation in Fig. 3 may prove to be fortuitous, or to be valid only for certain time periods. Taken at face value, however, the elevated reversal frequency observed for the last 30–40 Myr could imply that several plume heads left the CMB since that time and are now rising through the mid-mantle. Consequently, if this correlation could be made robust through a greater understanding of the mantle plume head generation and rise process, as well as the geodynamo's response to the resulting changes in CMB heat flow, the palaeomagnetic record could, in the future, perhaps help predict plume activity at the surface.

Potential links with true polar wander

The Earth's spin axis tends to align with the maximum non-hydrostatic inertia axis imposed by mantle density anomalies (including slabs, plumes and thermochemical piles) through TPW, a re-orientation of the entire Earth's mantle and crust relative to the spin axis[89]. The large-scale orientation of the outer core fluid motion is dictated by the spin axis, and therefore the main effect of TPW on the geodynamo is to change the pattern of heat flow across the CMB with respect to it. It is these changes in heat flow boundary conditions, rather than the rotations themselves, that possibly influence geomagnetic behaviour. TPW occurs at a rate determined by mantle viscosity of probably <~1–2 degrees Myr^{-1} (refs 90,91), and observations indicate that, during the past 300 Myr, TPW has moved the pole up to ~23° from its present location, roughly in a plane such that the two thermochemical piles beneath Africa and the Pacific remain close to the equator[92].

Except for one early study[7], little attention has been paid to how reported episodes of TPW could have influenced geomagnetic field behaviour. Presuming that the stability of the geodynamo is indeed sensitive to the spatial pattern of heat flow (and equatorial heat flow in particular), it could, however, be very important.

The effect (described by a kernel function) that density anomalies at different depths within the mantle have on the Earth's moment of inertia is likely to be such that TPW will tend to place dense slabs in the upper and upper-mid mantle at low latitudes and those in the lowermost mantle at higher latitudes[90]. The reverse is true of rising plume heads of low density. Because of these mutual compensations, it is difficult to obtain a good agreement between modelled and observation-based TPW, and therefore the results presented in Fig. 2 and Supplementary Fig. S1 do not consider the TPW that would follow from these models. Qualitatively, the combined effect of any major perturbation to subduction and/or plume flux (produced by, for example, supercontinent formation or breakup) that affects the degree 2 component of the geoid would be to cause patches of thinned TBL (elevated heat flux) produced by either slabs and/or plumes to move first towards the equator, and then towards the poles. We provide an exaggerated demonstration of this process in Fig. 4, which shows the response of the CMB heat flow in an equatorial zone (given as a fraction of the total heat flow) to episodes of TPW resulting from subduction being switched 'on' and 'off' in the model. After a delay of approximately 100 Myr, both of these perturbations cause episodes of TPW that produce dramatic rises and falls in the equatorial heat flow. Coupled to a sensitivity of the geodynamo to equatorial heat flow, this general process might implicate episodes of TPW as a contributor to observed episodes of reversal hyperactivity followed by superchrons in the palaeomagnetic record. Various dramatic episodes of TPW claimed for the early Phanerozoic and Proterozoic[93] have been linked to the supercontinent cycle, and could correspond to the earlier, relatively rapid, transitions in geomagnetic behaviour (Fig. 1b)[50,53] mentioned previously. More palaeomagnetic data from around these intervals would be useful to test this link.

Figure 5 shows the results of a simple analysis that applies four recently outlined episodes of TPW (refs 92,94) for the period 100–250 Myr ago to the SMEAN seismic tomography model at a depth slice of 2850 km (ref. 95). Assuming that the shear wave velocity anomaly at this depth can be used to infer variations in CMB heat flow[63], we find that, even in the absence of any temporal CMB variations in the mantle reference frame, the TPW rotations would have produced changes in equatorial heat flow that relate reasonably well in sign, relative amplitude and timing to those required to cause the observed geomagnetic changes in the same period. The same rotations, applied to an output of a mantle flow model, cause substantial changes (up to 40% for the ±10° latitude zone)

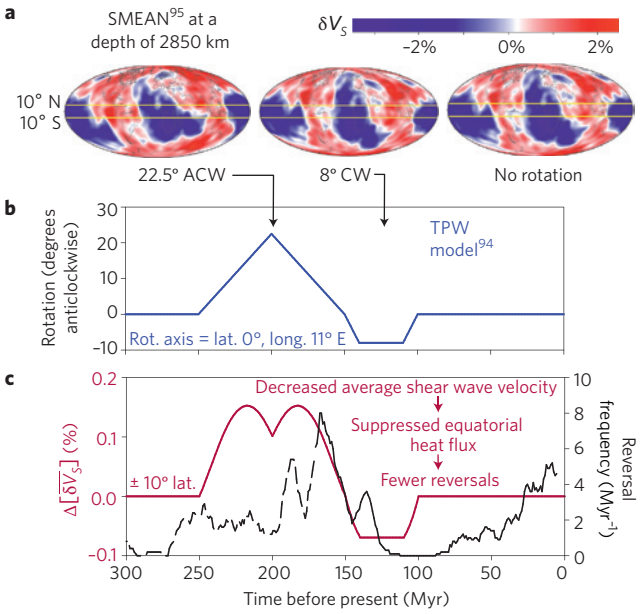

Figure 5 | Analysis of possible effects of observed TPW on equatorial CMB heat flow (and hence reversal frequency). a, Rotated examples of the SMEAN tomographic model[95]. Higher shear wave velocities (red areas) are likely to be associated with lower temperatures and higher CMB heat flux. **b**, Model of TPW for the last 300 Myr[94]. **c**, Resulting time series (red line) of variations in average shear wave velocity (inferring relative changes in heat flow) in the equatorial region (between 10° N and 10° S) shown alongside reversal frequency (black line).

in the equatorial heat flow (see Supplementary Information). We therefore conclude that, subject to the necessary sensitivity of the geodynamo being confirmed, TPW could well have contributed to changes in geomagnetic behaviour over this time period — particularly the reduction of reversal frequency and increase in mean dipole moment observed between the Middle Jurassic and Middle Cretaceous.

Links between the mantle and the geodynamo

Transitions in geomagnetic behaviour manifested primarily as decreases in average reversal frequency preceding superchrons may be caused by reductions in CMB heat flow globally, or in the equatorial region. The most recent such transition occurring between the Middle Jurassic and Middle Cretaceous coincided with a major TPW event that probably moved patches of high heat flow away from the equator. It may also have been associated with a decline in average mantle plume head production rate at the CMB that could have signified a decrease in the net heat flow across that boundary. The most recent long-term increase in average reversal frequency since the Late Cretaceous may have been caused by increasing equatorial asymmetry in CMB heat flow or another subduction-related process that triggered the departure of plume heads that have not yet reached the surface. These and other correlations are not mutually exclusive; slabs, plumes, dense basal piles and TPW are all interrelated elements of mantle convection[75,90,96]. This interrelation may provide any future successful overarching hypothesis with the opportunity to unify numerous different components of the core–mantle–crust system, as well as taking into account the time lags implicit between them.

The correlations outlined above fit our qualitative understanding of how the geodynamo is likely to respond to CMB heat flow changes, but are otherwise not yet robust. More comprehensive and realistic modelling studies aimed at better constraining the history of CMB heat flow, and the geodynamo's sensitivity to possible changes in it, are now required. Furthermore, the generic links outlined here should be tested using palaeomagnetic data describing geomagnetic behaviour and palaeogeography (including the position of the rotation axis) during earlier time periods.

References

1. Jonkers, A. R. T. Discrete scale invariance connects geodynamo timescales. *Geophys. J. Int.* **171,** 581–593 (2007).
2. Hulot, G. & Gallet, Y. Do superchrons occur without any palaeomagnetic warning? *Earth Planet. Sci. Lett.* **210,** 191–201 (2003).
3. Jonkers, A. R. T. Long-range dependence in the Cenozoic reversal record. *Phys. Earth Planet. Inter.* **135,** 253–266 (2003).
4. Jones, G. M. Thermal interaction of the core and the mantle and long-term behavior of the geomagnetic field. *J. Geophys Res* **82,** 1703–1709 (1977).
5. Mcfadden, P. L. & Merrill, R. T. Lower mantle convection and geomagnetism. *J. Geophys. Res.* **89,** 3354–3362 (1984).
6. Biggin, A. J. & Thomas, D. N. Analysis of long-term variations in the geomagnetic poloidal field intensity and evaluation of their relationship with global geodynamics. *Geophys. J. Int.* **152,** 392–415 (2003).
7. Courtillot, V. & Besse, J. Magnetic-field reversals, polar wander, and core-mantle coupling. *Science* **237,** 1140–1147 (1987).
8. Courtillot, V. & Olson, P. Mantle plumes link magnetic superchrons to Phanerozoic mass depletion events. *Earth Planet. Sci. Lett.* **260,** 495–504 (2007).
9. Eide, E. A. & Torsvik, T. H. Paleozoic supercontinental assembly, mantle flushing, and genesis of the Kiaman Superchron. *Earth Planet. Sci. Lett.* **144,** 389–402 (1996).
10. Gaffin, S. Phase difference between sea-level and magnetic reversal rate. *Nature* **329,** 816–819 (1987).
11. Haggerty, S. E. Superkimberlites — a geodynamic diamond window to the earths core. *Earth Planet. Sci. Lett.* **122,** 57–69 (1994).
12. Larson, R. L. & Kincaid, C. Onset of mid-Cretaceous volcanism by elevation of the 670 km thermal boundary layer. *Geology* **24,** 551–554 (1996).
13. Larson, R. L. & Olson, P. Mantle plumes control magnetic reversal frequency. *Earth Planet. Sci. Lett.* **107,** 437–447 (1991).
14. Pétrélis, F., Besse, J. & Valet, J.-P. Plate tectonics may control geomagnetic reversal frequency. *Geophys. Res. Lett.* **38,** L19303 (2011).
15. Zhang, N. & Zhong, S. J. Heat fluxes at the Earth's surface and core-mantle boundary since Pangea formation and their implications for the geomagnetic superchrons. *Earth Planet. Sci. Lett.* **306,** 205–216 (2011).
16. Ricou, L. E. & Gibert, D. The magnetic reversal sequence studied using wavelet analysis: a record of the Earth's tectonic history at the core-mantle boundary. *CR Acad. Sci. II A* **325,** 753–759 (1997).
17. Vogt, P. R. Evidence for global synchronism in mantle plume convection, and possible significance for geology. *Nature* **240,** 338–342 (1972).
18. Jones, G. M. Thermal interaction of core and mantle and long-term behavior of geomagnetic-field. *J. Geophys. Res.* **82,** 1703–1709 (1977).
19. Loper, D. E. & Mccartney, K. Mantle plumes and the periodicity of magnetic-field reversals. *Geophys. Res. Lett.* **13,** 1525–1528 (1986).
20. Torsvik, T. H., Burke, K., Steinberger, B., Webb, S. J. & Ashwal, L. D. Diamonds sampled by plumes from the core-mantle boundary. *Nature* **466,** 352–355 (2010).
21. Van der Meer, D. G., Spakman, W., van Hinsbergen, D. J. J., Amaru, M. L. & Torsvik, T. H. Towards absolute plate motions constrained by lower-mantle slab remnants. *Nature Geosci.* **3,** 36–40 (2010).
22. Constable, C. G. Modelling the geomagnetic field from syntheses of paleomagnetic data. *Phys. Earth Planet. Inter.* **187,** 109–117 (2011).
23. Korte, M. & Holme, R. On the persistence of geomagnetic flux lobes in global Holocene field models. *Phys. Earth Planet. Inter.* **182,** 179–186 (2010).
24. Hoffman, K. A. & Singer, B. S. Magnetic source separation in Earth's outer core. *Science* **321,** 1800–1800 (2008).
25. Christensen, U. R. Geodynamo models: Tools for understanding properties of Earth's magnetic field. *Phys. Earth Planet. Inter.* **187,** 157–169 (2011).
26. Kutzner, C. & Christensen, U. R. Simulated geomagnetic reversals and preferred virtual geomagnetic pole paths. *Geophys. J. Int.* **157,** 1105–1118 (2004).
27. Buffett, B. A. in *Core Dynamics* Vol. 8 *Treatise on Geophysics* (ed. Olson, P.) Ch. **12**, 345–358 (Elsevier, 2007).
28. Cande, S. C. & Kent, D. V. Revised calibration of the geomagnetic polarity timescale for the Late Cretaceous and Cenozoic. *J. Geophys. Res.-Sol. Ea.* **100,** 6093–6095 (1995).
29. Tominaga, M., Sager, W. W., Tivey, M. A. & Lee, S. M. Deep-tow magnetic anomaly study of the Pacific Jurassic Quiet Zone and implications for the geomagnetic polarity reversal timescale and geomagnetic field behavior. *J. Geophys. Res.-Sol. Ea.* **113,** B07110 (2008).

30. Sager, W. W., Weiss, C. J., Tivey, M. A. & Johnson, H. P. Geomagnetic polarity reversal model of deep-tow profiles from the Pacific Jurassic Quiet Zone. *J. Geophys. Res.-Sol. Ea.* **103,** 5269–5286 (1998).
31. Tominaga, M. & Sager, W. W. Revised Pacific M-anomaly geomagnetic polarity timescale. *Geophys. J. Int.* **182,** 203–232 (2010).
32. Gradstein, F. M., Ogg, J. G. & Smith, A. G. *A Geologic Time Scale 2004* 589 (Cambridge Univ. Press, 2004).
33. Ogg, J. G. in *A Geological Time Scale 2004* (eds Gradstein, F. M., Ogg, J. G. & Smith, A. G.) 307–339 (Cambridge Univ. Press, 2004).
34. Ogg, J. G., Coe, A. L., Przybylski, P. A. & Wright, J. K. Oxfordian magnetostratigraphy of Britain and its correlation to Tethyan regions and Pacific marine magnetic anomalies. *Earth Planet. Sci. Lett.* **289,** 433–448 (2010).
35. Gee, J. S. & Kent, D. V. in *Geomagnetism* Vol. 5 *Treatise on Geophysics* (ed. Kono, M.) Ch. **12**, 455–507 (Elsevier, 2007).
36. He, H., Pan, Y., Tauxe, L., Qin, H. & Zhu, R. Toward age determination of the M0r (Barremian–Aptian boundary) of the early Cretaceous. *Phys. Earth Planet. Inter.* **169,** 41–48 (2008).
37. Granot, R., Tauxe, L., Gee, J. S. & Ron, H. A view into the Cretaceous geomagnetic field from analysis of gabbros and submarine glasses. *Earth Planet. Sci. Lett.* **256,** 1–11 (2007).
38. Tauxe, L. & Yamazaki, T. in *Geomagnetism* Vol. 5 *Treatise on Geophysics* (ed Kono, M.) Ch. **13**, 510–563 (Elsevier, 2007).
39. Qin, H., He, H., Liu, Q. & Cai, S. Palaeointensity just at the onset of the Cretaceous normal superchron. *Phys. Earth Planet. Inter.* **187,** 199–211 (2011).
40. Tarduno, J. A. & Smirnov, A. V. in *Timescales of the Paleomagnetic Field* Vol. 145 *Geophys. Monogr. Series* (eds Channell, J. E. T., Kent, D. V., Lowrie, W. & Meert, J. G.) 328 (AGU, 2004).
41. Granot, R., Dyment, J. & Gallet, Y. Geomagnetic field variability during the Cretaceous Normal Superchron. *Nature Geosci.* **5,** 220–223 (2012).
42. Prévot, M., Derder, M. E., Mcwilliams, M. & Thompson, J. Intensity of the Earths magnetic-field — evidence for a Mesozoic dipole low. *Earth Planet. Sci. Lett.* **97,** 129–139 (1990).
43. Valet, J. P. Time variations in geomagnetic intensity. *Rev. Geophys* **41,** 1004 (2003).
44. Perrin, M. & Shcherbakov, V. Paleointensity of the earth's magnetic field for the past 400 Ma: Evidence for a dipole structure during the Mesozoic Low. *J. Geomagn. Geoelectr.* **49,** 601–614 (1997).
45. Tarduno, J. A. & Cottrell, R. D. Dipole strength and variation of the time-averaged reversing and nonreversing geodynamo based on Thellier analyses of single plagioclase crystals. *J. Geophys. Res. B-Sol. Earth* **110,** 1–10 (2005).
46. McElhinny, M. W. & Larson, R. L. Jurassic dipole low defined from land and sea data. *Eos Trans. AGU* **84,** 362 (2003).
47. Biggin, A. J., van Hinsbergen, D., Langereis, C. G., G. B., S. & Deenen, M. H. L. Geomagnetic secular variation in the Cretaceous Normal Superchron and in the Jurassic. *Phys. Earth Planet. Inter.* **169,** 3–19 (2008).
48. McFadden, P. L. & Merrill, R. T. Evolution of the geomagnetic reversal rate since 160 Ma: Is the process continuous? *J. Geophys. Res.-Sol. Ea.* **105,** 28455–28460 (2000).
49. Langereis, C. G., Krijgsman, W., Muttoni, G. & Menning, M. Magnetostratigraphy — concepts, definitions, and applications. *Newslett Stratigr.* **43,** 207–233 (2010).
50. Pavlov, V. & Gallet, Y. A third superchron during the Early Paleozoic. *Episodes* **28,** 78–84 (2005).
51. Pavlov, V. & Gallet, Y. Middle Cambrian high magnetic reversal frequency (Kulumbe River section, northwestern Siberia) and reversal behaviour during the Early Palaeozoic. *Earth Planet. Sci. Lett.* **185,** 173–183 (2001).
52. Kouchinsky, A. *et al.* The SPICE carbon isotope excursion in Siberia: a combined study of the upper Middle Cambrian-lowermost Ordovician Kulyumbe River section, northwestern Siberian Platform. *Geol. Mag.* **145,** 609–622 (2008).
53. Pavlov, V. & Gallet, Y. Variations in geomagnetic reversal frequency during the Earth's middle age. *Geochem. Geophys. Geosys.* **11,** Q01Z10 (2010).
54. Aubert, J., Labrosse, S. & Poitou, C. Modelling the palaeo-evolution of the geodynamo. *Geophys. J. Int.* **179,** 1414–1428 (2009).
55. Driscoll, P. & Olson, P. Effects of buoyancy and rotation on the polarity reversal frequency of gravitationally driven numerical dynamos. *Geophys. J. Int.* **178,** 1337–1350 (2009).
56. Driscoll, P. & Olson, P. Superchron cycles driven by variable core heat flow. *Geophys. Res. Lett.* **38,** L09304 (2011).
57. Olson, P. Gravitational dynamos and the low-frequency geomagnetic secular variation. *Proc. Natl Acad. Sci. USA* **105,** 20159–20166 (2007).
58. Wicht, J., Stellmach, S. & Harder, H. in *Handbook of Geomathematics* (eds Freeden, W., Nashed, M. Z. & Sonar, T.) (Springer, 2010).
59. Olson, P. & Christensen, U. R. Dipole moment scaling for convection-driven planetary dynamos. *Earth Planet. Sci. Lett.* **250,** 561–571 (2006).
60. Pozzo, M., Davies, C., Gubbins, D. & Alfè, D. Thermal and electrical conductivity of iron at Earth's core conditions. *Nature* **485,** 355–358 (2012).
61. Christensen, U. R. & Aubert, J. Scaling properties of convection-driven dynamos in rotating spherical shells and application to planetary magnetic fields. *Geophys. J. Int.* **166,** 97–114 (2006).
62. Glatzmaier, G. A., Coe, R. S., Hongre, L. & Roberts, P. H. The role of the Earth's mantle in controlling the frequency of geomagnetic reversals. *Nature* **401,** 885–890 (1999).
63. Olson, P. L., Coe, R. S., Driscoll, P. E., Glatzmaier, G. A. & Roberts, P. H. Geodynamo reversal frequency and heterogeneous core-mantle boundary heat flow. *Phys. Earth Planet. Inter.* **180,** 66–79 (2010).
64. Pétrélis, F., Fauve, S., Dormy, E. & Valet, J. P. Simple mechanism for reversals of Earth's magnetic field. *Phys. Rev. Lett.* **102,** 144503 (2009).
65. Wicht, J., Stellmach, S. & Harder, H. in *Geomagnetic field variations — Space–time structure, processes, and effects on system Earth.* (eds Glassmeier, K. H., Soffel, H. & Negendank, J.) 107–158 (Springer, 2009).
66. Lay, T., Hernlund, J. & Buffett, B. A. Core-mantle boundary heat flow. *Nature Geosci.* **1,** 25–32 (2008).
67. Van der Hilst, R. D. *et al.* Seismostratigraphy and thermal structure of Earth's core-mantle boundary region. *Science* **315,** 1813–1817 (2007).
68. Garnero, E. J., Lay, T. & McNamara, A. in *Plates, plumes, and planetary processes* Vol. 430 *Geol. Soc. Am. Special Paper* (eds Foulger, G. R. & Jurdy, D. M.) 79–101 (2007).
69. Machetel, P. & Thomassot, E. Cretaceous length of day perturbation by mantle avalanche. *Earth Planet. Sci. Lett.* **202,** 379–386 (2002).
70. Fukao, Y., Widiyantoro, S. & Obayashi, M. Stagnant slabs in the upper and lower mantle transition region. *Rev. Geophys.* **39,** 291–323 (2001).
71. Van der Voo, R., Spakman, W. & Bijwaard, H. Mesozoic subducted slabs under Siberia. *Nature* **397,** 246–249 (1999).
72. Van der Hilst, R. D., Widiyantoro, S. & Engdahl, E. R. Evidence for deep mantle circulation from global tomography. *Nature* **386,** 578–584 (1997).
73. Grand, S. P., Van der Hilst, R. D. & Widiyantoro, S. Global seismic tomography: A snapshot of convection in the Earth. *GSA Today* **7,** 1–7 (1997).
74. Goes, S., Capitanio, F. A. & Morra, G. Evidence of lower-mantle slab penetration phases in plate motions. *Nature* **451,** 981–984 (2008).
75. Steinberger, B. M. & Torsvik, T. H. A geodynamic model of plumes from the margins of large low shear velocity provinces. *Geochem. Geophys. Geosys.* **13,** Q01W09 (2012).
76. Čížková, H., van den Berg, A. P., Spakman, W. & Matyska, C. The viscosity of Earth´s lower mantle inferred from sinking speed of subducted lithosphere. *Phys. Earth Planet. Inter.* http://dx.doi.org/10.1016/j.pepi.2012.1002.1010 (in the press).
77. Labrosse, S. Hotspots, mantle plumes and core heat loss. *Earth Planet. Sci. Lett.* **199,** 147–156 (2002).
78. Gonnermann, H. M., Jellinek, A. M., Richards, M. A. & Manga, M. Modulation of mantle plumes and heat flow at the core mantle boundary by plate-scale flow: results from laboratory experiments. *Earth Planet. Sci. Lett.* **226,** 53–67 (2004).
79. Nakagawa, T. & Tackley, P. J. Deep mantle heat flow and thermal evolution of the Earth's core in thermochemical multiphase models of mantle convection. *Geochem. Geophys. Geosys.* **6,** Q08003 (2005).
80. Thorne, M. S., Garnero, E. J. & Grand, S. P. Geographic correlation between hot spots and deep mantle lateral shear-wave velocity gradients. *Phys. Earth Planet. Inter.* **146,** 47–63 (2004).
81. Tan, E., Leng, W., Zhong, S. J. & Gurnis, M. On the location of plumes and lateral movement of thermochemical structures with high bulk modulus in the 3-D compressible mantle. *Geochem. Geophys. Geosys.* **12,** Q07005 (2011).
82. Burke, K., Steinberger, B., Torsvik, T. H. & Smethurst, M. A. Plume generation zones at the margins of large low shear velocity provinces on the core-mantle boundary. *Earth Planet. Sici. Lett.* **265,** 49–60 (2008).
83. Burke, K. Plate tectonics, the Wilson Cycle, and mantle plumes: geodynamics from the top. *Annu. Rev. Earth Planet. Sci.* **39,** 1–29 (2011).
84. Larson, R. L. Latest pulse of Earth — evidence for a midcretaceous superplume. *Geology* **19,** 547–550 (1991).
85. Bryan, S. E. & Ernst, R. E. Revised definition of large igneous provinces (LIPs). *Earth-Sci. Rev.* **86,** 175–202 (2008).
86. Olson, P., Schubert, G. & Anderson, C. Plume formation in the D-layer and the roughness of the core mantle boundary. *Nature* **327,** 409–413 (1987).
87. Thompson, P. F. & Tackley, P. J. Generation of mega-plumes from the core-mantle boundary in a compressible mantle with temperature-dependent viscosity. *Geophys. Res. Lett.* **25,** 1999–2002 (1998).
88. Van Hinsbergen, D. J. J., Steinberger, B., Doubrovine, P. V. & Gassmoller, R. Acceleration and deceleration of India-Asia convergence since the Cretaceous: Roles of mantle plumes and continental collision. *J. Geophys. Res.-Sol. Ea.* **116,** B06101 (2011).
89. Gold, T. Instability of the Earths axis of rotation. *Nature* **175,** 526–529 (1955).
90. Steinberger, B. & Torsvik, T. H. Toward an explanation for the present and past locations of the poles. *Geochem. Geophys. Geosys.* **11,** Q06W06 (2010).

91. Tsai, V. C. & Stevenson, D. J. Theoretical constraints on true polar wander. *J. Geophys. Res.-Sol. Ea.* **112,** B05415 (2007).
92. Steinberger, B. & Torsvik, T. H. Absolute plate motions and true polar wander in the absence of hotspot tracks. *Nature* **452,** 620–626 (2008).
93. Mitchell, R. N., Kilian, T. M. & Evans, D. A. D. Supercontinent cycles and the calculation of absolute palaeolongitude in deep time. *Nature* **482,** 208–296 (2012).
94. Torsvik, T. H. *et al.* Phanerozoic polar wander, paleogeography and dynamics. *Earth-Sci. Rev.* http://dx.doi.org/10.1016/j.earscirev.2012.06.007 (2012).
95. Becker, T. W. & Boschi, L. A comparison of tomographic and geodynamic mantle models. *Geochem. Geophys. Geosys.* **3,** 1003 (2002).
96. Tan, E., Gurnis, M. & Han, L. J. Slabs in the lower mantle and their modulation of plume formation. *Geochem. Geophys. Geosys.* **3,** 1067 (2002).
97. Biggin, A., McCormack, A. & Roberts, A. Paleointensity database updated and upgraded. *Eos Trans. AGU* **91,** 15 (2010).
98. Thellier, E. & Thellier, O. Sur l'intensité du champ magnétique terrestre dans la passé historique et géologique. *Ann. Géophys.* **15,** 285–376 (1959).
99. Hill, M. J. & Shaw, J. Magnetic field intensity study of the 1960 Kilauea lava flow, Hawaii, using the microwave palaeointensity technique. *Geophys. J. Int.* **142,** 487–504 (2000).
100. Yamamoto, Y., Tsunakawa, H. & Shibuya, H. Palaeointensity study of the Hawaiian 1960 lava: implications for possible causes of erroneously high intensities. *Geophys. J. Int.* **153,** 263–276 (2003).

Acknowledgements

A.J.B. is funded by a NERC Advanced Fellowship (NE/F015208/1). N.S., A.J.B. and R.H. are funded by a NERC standard grant (NE/H021043/1). A.J.B. acknowledges valuable discussions with Neil Thomas and Mimi Hill. J.A. acknowledges support from program PNP/SEDI-TPS of French Instutut National des Sciences de l'Univers (INSU). T.H.T. acknowledges the European Research Council for financial support.

Author Contributions

A.J.B., B.S. and J.A. prepared the text with contributions from all other authors. B.S. supplied the mantle modelling results. New analyses were performed by A.J.B and B.S. All authors contributed to discussions about the ideas presented.

Additional information

The authors declare no competing financial interests. Supplementary information accompanies this paper on www.nature.com/naturegeoscience. Correspondence and requests for materials should be addressed to A.J.B.

CORRIGENDUM

Possible links between long-term geomagnetic variations and whole-mantle convection processes

A. J. Biggin, B. Steinberger, J. Aubert, N. Suttie, R. Holme, T. H. Torsvik, D. G. van der Meer and D. J. J. van Hinsbergen

Published online: 29 July 2012 | http://dx.doi.org/10.1038/ngeo1521

In the print version of this Review article, some labelling in Figs 3, 4a and 5c is incorrect: in Fig. 3 the label 'Laurrassia and Gondwana collide' is incorrectly placed; in Fig. 4a some axes labels were incorrect; in Fig. 5c the Greek δ symbol has printed incorrectly. All figures are correct online.